Metabolic Kinetics of a Glioma Model Using Hyperpolarized 13C Magnetic Resonance Spectroscopic Imaging

J. Park[1,2], S. Josan[2,3], T. Jang[4], M. Merchant[4], Y-F. Yen[5], R. Hurd[5], L. Recht[4], D. Spielman[1,2], and D. Mayer[2,3]

[1]Department of Electrical Engineering, Stanford University, Stanford, CA, United States, [2]Department of Radiology, Stanford University, Stanford, CA, United States, [3]SRI International, Menlo Park, CA, United States, [4]Department of Neurology and Neurological Sciences, Stanford University, Stanford, CA, United States, [5]Global Applied Science Laboratory, GE Healthcare, Menlo Park, CA, United States

Introduction: ^{13}C magnetic resonance spectroscopy (MRS) has been used to study *in vivo* tumor metabolism in brain tumor models, and the altered energy metabolism is marked by the elevated production of ^{13}C-labeled lactate (Lac) in tumor tissue [1]. Dynamic nuclear polarization (DNP) and the recent development of a dissolution process that retains polarization in the liquid state enables a real-time investigation of *in vivo* metabolism with more than a 10,000-fold signal increase over conventional ^{13}C methods [2]. Recently, a study showed the feasibility of using hyperpolarized [1-^{13}C]-pyruvate (Pyr) for evaluating *in vivo* metabolism of a human glioblastoma xenograft in a rat brain at a single time point [3]. In this work, we measured the kinetics of pyruvate metabolism in a glioma brain tumor model using the hyperpolarized ^{13}C technique with a fast spiral chemical shift imaging (CSI) [4] sequence, and compared the metabolic kinetics from three different region of interests (ROIs): brain tumor, normal brain, and vasculature.

Method: All measurements were performed on a clinical 3-T MR scanner with a high-performance insert gradient coil (500mT/m, 1,800mT/ms, 160mm inner diameter). A custom-built dual-tuned ($^{1}H/^{13}C$) quadrature rat coil (Ø=50mm) was used for both RF excitation and signal reception. Approximately 10^6 C6 rat glioma cells, derived from a nitrosourea-induced tumor, were implanted into the brains of adult female Sprague-Dawley rats (n=3) nine days prior to the ^{13}C experiment. The tumors grow rapidly after implantation, generally resulting in symptoms requiring euthanasia by day 15. The implanted rats (200-250 g weight) were anesthetized with 1-3% isoflurane in oxygen (~1.5L/min), and were injected through their tail veins with 2.5-3.0 mL of 80mM solution of [1-^{13}C] pyruvate that had been hyperpolarized using HyperSense DNP (15-20% liquid-state polarization). The fast spiral CSI sequence used a variable flip angle leading upto 90° over 16 time points with TR = 3 s, slice thickness = 5 mm, and a 2.7-mm in-plane spatial resolution. Multiple injections (2-3) per animal were performed to increase signal-to-noise ratio (SNR). The slice showing the biggest tumor was carefully selected from the T_2-weighted ^{1}H images, and gadolinium-enhanced T_1-weighted ^{1}H images were obtained after ^{13}C experiments to confirm the tumor location. After correcting for RF flip angles, the temporal dynamic curve of each ROI was fitted using a two-site exchange model [5, 6]; the fitting algorithm included parameters corresponding to T_1 losses, RF-sampling, an estimate of the time that a given spin resides in the RF excitation bandwidth, and metabolic rate constants.

Result: Figure 1 shows the time-averaged metabolic images of Pyr and Lac acquired from a representative rat (RatC6_2) using the spiral CSI pulse sequence. To maximize the contrast-to-noise ratio (CNR), the normalized time course from the glioma ROI was used to compute weighted-average images. Each metabolic image was superimposed onto a Gd-enhanced ^{1}H spin echo image (1-mm slice) for anatomical reference. Histology corresponding to the scanned slice confirmed the size and location of glioma. The time courses of Pyr and Lac from the regions of glioma, normal brain, and blood vessel are shown in Figure 2. Table 1 summarizes the apparent rate constants with χ^2 statistic for the fit and CNR of all 3 rats. The apparent rate constant of Pyr-to-Lac conversion, $k_{pyr\rightarrow lac}$, in the brain tumor was noticeably higher than that in the normal brain and the vasculature: (0.017 ± 0.0045) s^{-1} in glioma, (0.011 ± 0.0015) s^{-1} in normal brain, (0.0049 ± 0.00012) s^{-1} in vasculature. CNR was calculated from the averaged lactate signal difference of glioma and normal brain ROIs divided by the background noise.

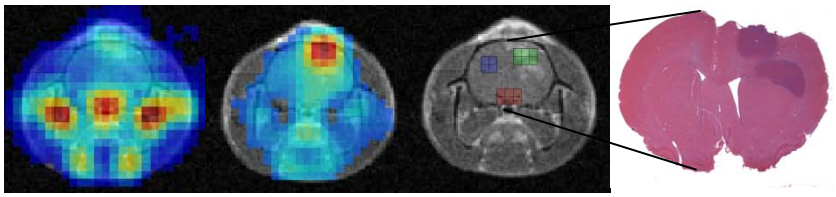

Figure 1: Time-averaged metabolic images of (A) Pyr and (B) Lac computed from three 2D dynamics studies on the same rat (RatC6_2). (C) Voxels selected for ROI analysis: Tumor (Green), Normal brain (Blue), Vasculature (Red). (D) The histology image of the scanned slice.

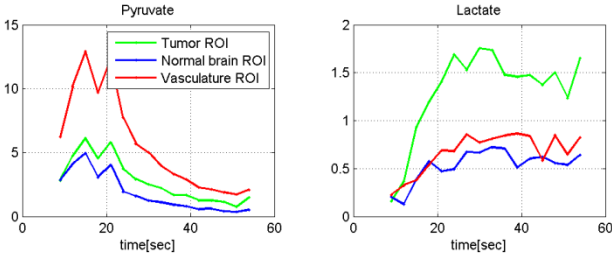

Figure 2: Representative time course of Pyr and Lac in tumor, normal brain, and vasculature regions from the average of three injections for subject C6_2.

	Number of Injection	CNR	$K_{Pyr\rightarrow Lac}$ in s^{-1} (χ^2)		
			Glioma	Normal Brain	Vasculature
RatC6_1	2	19.40	0.013 (0.019)	0.010 (0.071)	0.005 (0.034)
RatC6_2	3	33.69	0.022 (0.0070)	0.011 (0.017)	0.0048 (0.019)
RatC6_4	2	16.81	0.017 (0.047)	0.013 (0.059)	0.005 (0.028)

Table 1: Comparison of CNR and apparent rate constants from each rat.

Discussion: *In vivo* results clearly demonstrated the difference in kinetics of the brain tumor metabolism in comparison to those of normal brain and vasculature. The Pyr signal also provided an estimate of tissue perfusion, in which blood-brain barrier breakdown in the tumor results in the Pyr curve from the tumor ROI approaching that from the vascular ROI in some animals. The tumor ROI was also close to a sagittal sinus, which also contributes to higher Pyr signal due to the relatively low spatial resolution. Robust dynamic curves of Pyr and Lac were achievable repeatedly with 3 seconds of temporal resolution using the variable RF excitation angle on a single slice, whereas bicarbonate signal detection was limited by the SNR. We also imaged with a recently developed dynamic volumetric spiral CSI sequence covering the entire brain (n=1), with and without additional ^{12}C-Lac in the dissolution buffer. In Lac images, SNR of glioma ROI and CNR were improved by 20.0 %, and 37.3 % respectively compared to those obtained with a normal NaOH buffer, identifying isotopic exchange as an important process in ^{13}C-Lac labeling.

References: [1] Terpstra, M., et al, *Cancer Res* 1998; 58(22):5083-5088, [2] Golman, K., et al, *Cancer Res*. 2006; 66:10855-10860, [3] Park, I., et al, *Neuro-Oncology* 2010; 12:133-144, [4] Mayer, D., et al, *MRM* 2009; 62:557, [5] Zierhut, D., et al, *MRM* 2010; 202:85-92, [6] Day, S., et al, *Nature Med* 2007; 13:1382-1387

Acknowledgements: **NIH**: RR09784, AA05965, AA018681, AA13521-INIA, and EB009070, **The Lucas Foundation**, and **GE Healthcare**